Pervaporation Separation of Water–Acetic Acid Mixtures Through NaY Zeolite-Incorporated Sodium Alginate Membranes

A. A. Kittur, S. M. Tambe, S. S. Kulkarni, M. Y. Kariduraganavar

Department of Chemistry and Center of Excellence in Polymer Science, Karnatak University, Dharwad 580 003, India

Received 5 April 2004; accepted 11 June 2004
DOI 10.1002/app.21149
Published online in Wiley InterScience (www.interscience.wiley.com).

ABSTRACT: The pervaporation (PV) separation and swelling behavior of water–acetic acid mixtures were investigated at 30, 40, and 50°C using pure sodium alginate and its zeolite-incorporated membranes. The effects of zeolite loading and feed composition on the pervaporation performance of the membranes were analyzed. Both the permeation flux and selectivity increased simultaneously with increasing zeolite content in the polymer matrix. This was discussed on the basis of a significant enhancement of hydrophilicity, selective adsorption, and molecular sieving action, including a reduction of pore size of the membrane matrix. The membrane containing 30 mass % of zeolite showed the highest separation selectivity of 42.29 with a flux of 3.80×10^{-2} kg m^{-2} h^{-1} at 30°C for 5 mass % of water in the feed. From the temperature dependency of diffusion and permeation data, the Arrhenius activation parameters were estimated. The E_p and E_D values ranged between 72.28 and 78.16, and 70.95 and 77.38 kJ/mol, respectively. The almost equal magnitude obtained in E_p and E_D values signified that both permeation and diffusion contribute equally to the PV process. All the membranes exhibited positive ΔH_s values, suggesting that the heat of sorption is dominated by Henry's mode of sorption. © 2004 Wiley Periodicals, Inc. J Appl Polym Sci 94: 2101–2109, 2004

Key words: separation techniques; membranes; zeolites; selectivity; activation energy

INTRODUCTION

Membrane-separation techniques, with an easy operation and high energy savings, are greatly appreciated in a variety of applications in the medical, food, industrial, energy, and environment fields.[1] Pervaporation (PV) is also a membrane-based technique in which the membrane functions as a selective barrier for the mixture to be separated. Because of low energy consumption and mild working conditions, PV becomes a promising process in the chemical industry for the separation of azeotropic mixtures, close boiling mixtures, and dehydration of temperature-sensitive products.[2–4]

The research efforts on the pervaporation process have been mainly concentrated on the separation of alcohol–water systems, but the separation of acetic acid–water systems has received relatively less attention.[5,6] Acetic acid is an important basic chemical in the chemical industry, ranking among the top 20 organic intermediates. The current processes for acetic acid production include the carbonylation of methanol, the liquid–phase oxidation of hydrocarbons, and the oxidation of acetaldehyde. One process for reducing the cost of acetic acid is fermentation of biomass, forestry residues, municipal wastes, and other byproducts.[7] The concentration of acetic acid obtained in this process is usually lower than 5 wt %.[8,9] Azeotropic distillation and extractive distillation have been developed for acetic acid recovery, but distillation is energy-intensive because of the small differences in the volatilities of water and acetic acid in dilute aqueous solution.[10,11] However, PV has the potential to separate acetic acid from aqueous mixtures because the chemical potential gradient across the membrane is the driving force for mass transport.

Sodium alginate (SA) is a membrane material with potential applications in dehydrating organic aqueous solutions. As known, its performance exceeds that of poly(vinyl alcohol) (PVA),[12] ion-exchange resins,[13] and some other polysaccharides with similar chemical structures such as chitosan[14] and cellulose.[15] This is the reason that SA is a prospective membrane material that can be applied in treating organic solvents, which are of great economic value in medical and agrochemical industries. However, the performance of a pure SA membrane is still not satisfactory because of a large

Correspondence to: M. Y. Kariduraganavar (mahadevappak@yahoo.com).

Contract grant sponsor: Department of Science and Technology, New Delhi; contract grant number: SP/S1/H-31/2000.

free volume between the molecular chains.[16] Its membrane performance has been improved by modifying alginate with different methods such as blending,[17,18] grafting,[19] and crosslinking.[20,21] Alternatively, incorporation of highly selective zeolite into the membrane matrix can also be effective. For instance, Gao et al.[22] and Chen et al.,[16] respectively, studied the pervaporation separation of hydrophilic zeolite-filled PVA and chitosan membranes for organic–water systems. The incorporation of such zeolites or porous fillers in dense membranes can improve the separation performance of the membrane[23–25] as the result of the combined effects of molecular sieving action, selective adsorption, and difference in diffusion rates. In addition, zeolites have high mechanical strength and good thermal and chemical stability; thus, the membranes incorporated with zeolites can be used over a wide range of operating conditions.

In the PV process, the simultaneous enhancement of both selectivity and flux has been a big challenge as a consequence of a trade-off phenomenon, existing between flux and selectivity, although much research effort is being continued to overcome the situation by enhancing the hydrophilicity of the membrane by different methods such as γ-irradiation, chemical grafting, and plasma deposition.[4,26,27] Recently, we succeeded in increasing both selectivity and flux by judiciously incorporating different amounts of suitable hydrophilic zeolite into SA membranes for the separation of water–isopropanol mixtures.[25]

In continuation, the pervaporation study is now extended for the separation of water–acetic acid mixtures at 30, 40, and 50°C. The values of permeation flux, separation selectivity, and diffusion coefficient were evaluated. From the temperature dependency of the permeation flux and diffusion coefficient data, the Arrhenius activation parameters were estimated. These results are discussed in terms of the PV separation ability of the membranes.

EXPERIMENTAL

Materials

Sodium alginate (SA) and acetic acid (HAc) were purchased, respectively, from Luba Chemicals (Mumbai, India) and S. D. Fine Chemicals (Mumbai, India). NaY zeolite was kindly supplied by Indian Petrochemicals Corp. (Baroda, India). All the chemicals were of reagent grade and used without further purification. Double-distilled water was used throughout the research work.

Membrane preparation

Sodium alginate (4 g) was dissolved in 100 mL of deaerated distilled water with constant stirring for about 24 h at room temperature. It was then filtered and the resulting solution was cast onto a glass plate with the aid of a casting knife. The membrane was allowed to dry at room temperature for 2–3 days. The completely dried membrane was subsequently peeled off and was designated as M.

To prepare zeolite-filled SA membrane, a known amount of NaY zeolite was added to a same amount of SA solution. The solution was stirred for about 2 h and then was kept in an ultrasonic bath for about 30 min to break the aggregated crystals of zeolite and to improve the dispersion in the polymer matrix. The resulting homogeneous solution was poured onto a glass plate and the membrane was dried as mentioned above. The amount of NaY zeolite with respect to SA varied from 5 to 15 to 30 mass %, and the resulting membranes were designated as M-1, M-2, and M-3, respectively. The thickness of these membranes was measured at different points using a Peacock dial thickness gauge (Model G, Ozaki Mfg. Co., Japan) with an accuracy of ± 5 μm and the average thickness ($\sim$ 40 μm) was considered for calculation. The physical and spectroscopic properties of the derivatized membranes, in relation to their structure variation, were as described earlier.[25]

Pervaporation experiments

PV experiments were performed using an indigenously designed apparatus, illustrated in Figure 1(a) and (b). The effective area of the membrane in contact with the feed mixture was 34.23 cm^2 and the capacity of the feed compartment was about 250 cm^3. The vacuum in the downstream side of the apparatus was maintained (10 Torr) in all the experiments using a two-stage vacuum pump (Toshniwal, Chennai, India). The test membrane was allowed to equilibrate for about 1 h while in contact with the feed mixture before performing the experiment. After a steady state was attained, the experiments were carried out at 30, 40, and 50°C, and the permeate was collected in a trap immersed in the liquid nitrogen jar on the downstream side. The water composition in the feed varied between 5 and 25 mass %. The flux was calculated by weighing the permeate and its composition was estimated by measuring the refractive index of the mixture within an accuracy of ± 0.0001 units using a refractometer (Atago-3T, Tokyo, Japan), and by comparing it with a standard graph that was established with the known compositions of water–acetic acid mixtures.

Membrane performance in PV experiments was studied by calculating the total flux (J), separation factor (α_{sep}), and pervaporation separation index (PSI). These were calculated, respectively, using the following equations:

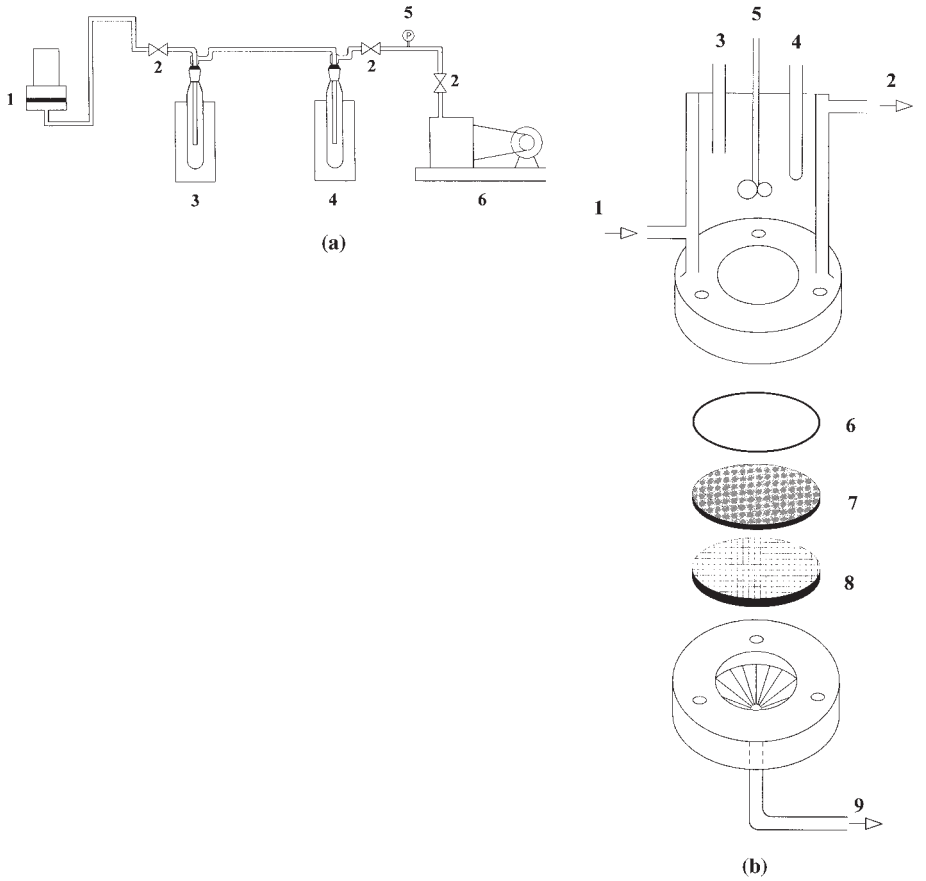

Figure 1 (a) Schematic representation of pervaporation apparatus: (1) pervaporation cell; (2) vacuum control valve; (3) permeate cold trap; (4) moisture cold trap; (5) pressure sensor; (6) vacuum pump. (b) Schematic diagram of pervaporation cell: (1) water inlet; (2) water outlet; (3) feed inlet; (4) thermometer jacket; (5) stirrer; (6) O-ring; (7) membrane; (8) sintered disk; (9) permeate outlet.

$$J = \frac{W}{At} \tag{1}$$

$$\alpha_{sep} = \frac{P_w / P_{HAc}}{F_w / F_{HAc}} \tag{2}$$

$$\text{PSI} = J(\alpha_{sep} - 1) \tag{3}$$

where W is the mass of permeate (kg); A is the effective area of the membrane (m^2); t is the permeation time (h); P and F are the mass percentages of permeate and feed, respectively; subscripts w and HAc denote water and acetic acid, respectively. The results of permeation for water–acetic acid mixtures during the pervaporation were reproducible within the admissible range.

Swelling measurements

The degree of swelling of membranes was carried out with different compositions of water–acetic acid mixtures using an electronically controlled oven (WTB Binder, Jena, Germany). The masses of the dry membranes were first determined and these were equilibrated by soaking in different compositions of the feed mixtures in a sealed vessel at 30°C for 24 h. The swollen membranes were weighed as quickly as possible after careful blotting on a digital microbalance (Model B204-S; Mettler–Toledo International, Zurich, Switzerland) having a sensitivity of ±0.01 mg. The percentage degree of swelling (DS) was calculated as

$$\text{DS}(\%) = \left(\frac{W_s - W_d}{W_d}\right) \times 100 \tag{4}$$

where W_s and W_d are the masses of the swollen and dry membranes, respectively.

RESULTS AND DISCUSSION

Effects of feed composition and zeolite loading on membrane swelling

It has been realized since the pioneering work of Flory and Rehner, reported in the early 1950s, that polymer swelling in certain liquids depends on various param-

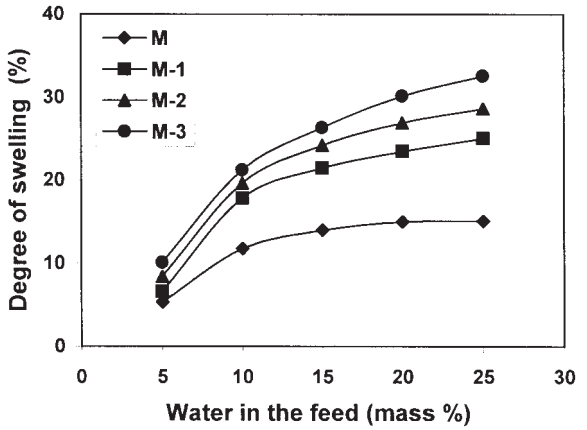

Figure 2 Variation of degree of swelling with different mass % of water in the feed at 30°C for different membranes.

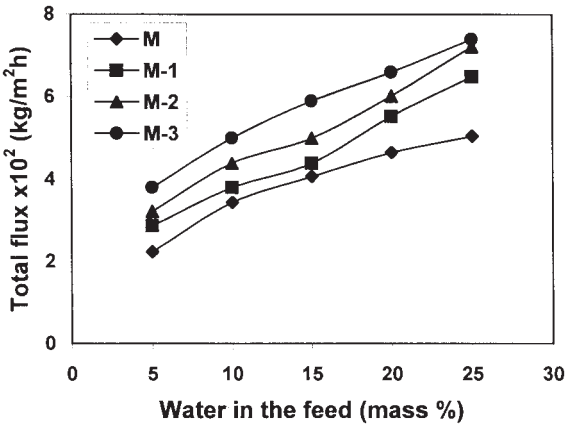

Figure 3 Variation of total flux with different mass % of water in the feed at 30°C for different membranes.

eters, such as chemical composition and microstructure of the polymer, and incorporated moiety, which strongly influence the water-sorption mechanism. In the PV experiment, membrane swelling is an important factor that controls the transport of permeating molecules under the chemical potential gradient.

In an effort to study the effects of feed composition and zeolite loading on membrane swelling, the percentage degree of swelling of all the membranes was plotted as a function of different mass % of water in the feed at 30°C, as shown in Figure 2. It is observed that the degree of swelling increased exponentially for all the membranes with increasing mass % of water in the feed. This is attributed to strong interactions between the hydroxyl and COO^- groups of SA with the water molecules. As the water concentration increased in the feed, the interaction with water becomes more predominant, given that water causes a greater degree of swelling than that of acetic acid with the membrane.

On the other hand, when the polymer matrices are filled with highly symmetrical zeolite particles, then it is likely that the pores of the membranes might have been occupied by the zeolite particles. This leads to an increased degree of swelling over that of the pure SA membrane, as observed in Figure 2. However, the effect is significantly increased from membrane M-1 to M-3 with increasing zeolite content. This is mainly because of the hydrophilic nature of the incorporated NaY zeolite in the membrane matrix. Besides, the incorporated NaY zeolite contains Na^+ ions in its channels, which tend to increase the electrostatic force of attraction between the water molecules and membrane. Thus, these combined properties substantially increase the adsorption of water molecules, resulting in greater swelling with increasing zeolite content in the membrane.

Effects of feed composition and zeolite loading on pervaporation

To study the effects of feed composition and zeolite loading on the permeation, the total permeation flux was plotted for all the membranes as a function of different mass % of water in the feed, as shown in Figure 3. It is observed that the total permeation flux increased almost linearly for all the zeolite-incorporated SA membranes with increasing amounts of water in the feed, attributed to an increase of selective interactions between water molecules and zeolite-incorporated SA membrane. However, for the pure SA membrane (M), the permeation flux increased linearly up to 10 mass % of water in the feed and, beyond this, the permeation flux increased exponentially. This may be the result of attaining the saturation of interactive groups (COO^- and OH) of sodium alginate with increasing water concentration in the feed. However, this phenomenon does not occur with the zeolite-incorporated SA membranes, wherein the increase of

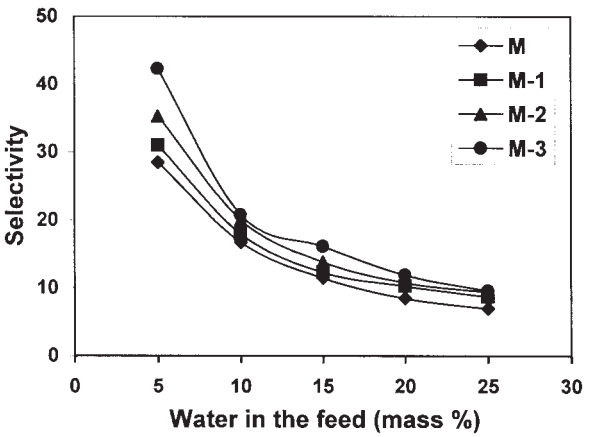

Figure 4 Variation of separation selectivity with different mass % of water in the feed at 30°C for different membranes.

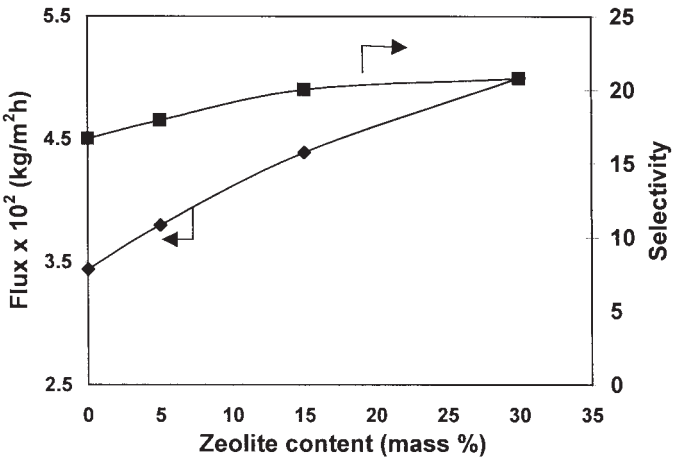

Figure 5 Variation of total flux and selectivity with different mass % of zeolite-incorporated membranes at 10 mass % of water in the feed.

NaY zeolite content in membrane enhances the selective interactions between the water molecules and the membrane. This is mainly attributed to the combined influence of ionic species (Na^+) present in the zeolite cages and porous nature of zeolite, apart from the hydrophilic nature of the membrane material. These together are responsible for the higher permeation flux with increasing water concentration in the feed, as evidenced by swelling study.

Overall selectivity of a membrane in the PV process is generally determined on the basis of interaction between the membrane and permeating molecules, molecular size of the permeating species, and pore diameter of the membrane. Figure 4 displays the effects of water composition and zeolite loading on selectivity of the membranes. It is observed that the selectivity decreased monotonically for all the membranes with increasing water concentration in the feed, attributed to greater swelling with increasing water concentration in the feed because of an increase of selective interaction between the membrane and water molecules. On the contrary, the selectivity increased from membrane M to M-3 upon increasing the NaY zeolite content in the membrane throughout the investigated range of water compositions. This is attributed to the increased selective interactions with increasing zeolite content in the membrane matrix. Further, it can be clearly observed from Figure 5, in which the flux and selectivity were plotted as a function of zeolite content in the membrane at 10 mass % of water in the feed. It is noticed that both the permeation flux and selectivity increased with increasing zeolite content in the membrane. Generally, by increasing the packing density of the membrane, either by increasing the crosslinking density or by incorporating the zeolite in the polymer matrix, the permeation flux decreases and selectivity increases because of a reduction of pore size within the membrane matrix.[2,18,19] In the present study, however, both the permeation flux and selectivity increased simultaneously with increasing packing density. Although this is in contrast to the trade-off phenomenon, frequently encountered between flux and separation factor in PV process, a significant enhancement of hydrophilicity, selective adsorption, and molecular sieving action overcome the situation by introducing porous zeolite-containing ionic particles in the membrane matrix.[25]

The results of total flux, selectivity, and fluxes of water and acetic acid, measured at 30°C for all the membranes in the investigated feed compositions, are

TABLE I
Pervaporation Flux and Separation Selectivity Data for Different Mass % of Water in the Feed at 30°C for Different Membranes

Mass % of water	$J \times 10^2$ (kg m^{-2} h^{-1})				α_{sep}			
	M	M-1	M-2	M-3	M	M-1	M-2	M-3
5	2.24	2.87	3.22	3.80	28.50	31.00	35.29	42.29
10	3.44	3.80	4.39	5.00	16.71	17.95	20.03	20.80
15	4.07	4.39	5.00	5.90	11.51	12.32	13.87	16.13
20	4.65	5.53	6.02	6.60	8.50	10.29	10.81	11.94
25	5.05	6.49	7.22	7.40	7.00	8.76	9.45	9.61

TABLE II
Pervaporation Fluxes of Water and Acetic Acid at Different Mass % of Water in the Feed at 30°C for Different Membranes

Mass % of water	$J_w \times 10^2$ (kg m^{-2} h^{-1})				$J_{HAC} \times 10^2$ (kg m^{-2} h^{-1})			
	M	M-1	M-2	M-3	M	M-1	M-2	M-3
5	1.34	1.77	2.09	2.62	0.89	1.09	1.13	1.18
10	2.24	2.53	3.03	3.49	1.20	1.27	1.36	1.51
15	2.73	3.01	3.55	4.36	1.34	1.38	1.45	1.53
20	3.17	3.98	4.39	4.94	1.49	1.55	1.63	1.66
25	3.53	4.83	5.48	5.64	1.51	1.65	1.74	1.76

presented in Tables I and II, respectively. It is observed that there is a systematic increase of total flux and fluxes of water and acetic acid with increasing amounts of zeolite and feed composition. Similarly, the selectivity increased systematically with increasing amount of zeolite throughout the investigated range of water composition, indicating that the addition of zeolite increases the selectivity of the membranes.

Pervaporation separation index (PSI)

Pervaporation separation index (PSI), defined as the product of total permeation and separation factor, has been used as a performance-evaluating parameter. Figure 6 shows the variation of PSI as a function of zeolite content in the membrane at 30°C for 10 mass % of water in the feed. It is observed that the PSI values increased almost linearly with increasing zeolite content, signifying that the membranes incorporated with a higher amount of zeolite showed better performance for the separation of acetic acid–water mixtures, attributed to the incorporation of zeolite into a membrane matrix that changes not only the membrane's hydrophilicity but also its structure, which may have a significant influence on diffusion. Sorption is only the first step but in the second step (diffusion), the different properties of zeolite and their significant role in the membrane improve the overall pervaporation performance.

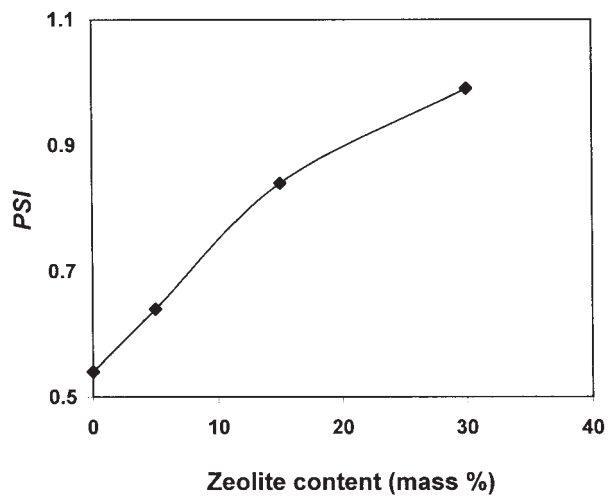

Figure 6 Variation of pervaporation separation index with different mass % of zeolite-incorporated membranes at 10 mass % of water in the feed.

Diffusion coefficient

Transport of binary liquid molecules in PV experiments is generally explained by the solution–diffusion mechanism, which occurs in three steps: sorption, diffusion, and evaporation.[28] Thus, the permeation rates and selectivity are governed by the solubility and diffusivity of each component of the feed mixture to be separated. In the process, because of establishing the fast equilibrium distribution between the bulk feed and the upstream surface of a membrane,[29,30] the diffusion step controls the migration of penetrants. Therefore, it is important to estimate the diffusion coefficient D_i of penetrating molecules to understand the transport mechanism.

From Fick's law of diffusion, the diffusion flux can be expressed as[31]

$$J_i = -D_i \frac{dC_i}{dx} \tag{5}$$

where J is the permeation flux per unit area (kg m^{-2} s^{-1}), D is the diffusion coefficient (m^2/s), C is the concentration of the permeate (kg/m^3), subscript i stands for water or acetic acid, and x is the diffusion length (m). For simplicity, it is assumed that the concentration profile along the diffusion length is linear. Therefore, the diffusion coefficient can be calculated using the following equation[32]:

$$D_i = \frac{J_i \delta}{C_i} \tag{6}$$

where δ is the membrane thickness. The calculated values of D_i at 30°C are presented in Table III. Similar

TABLE III
Diffusion Coefficients of Water and Acetic Acid Calculated from Eq. 6 at Different Mass % of Water in the Feed for Different Membranes

Mass % of water	$D_w \times 10^8$ (m^2/s)				$D_{HAc} \times 10^8$ (m^2/s)			
	M	M-1	M-2	M-3	M	M-1	M-2	M-3
5	5.41	7.19	8.49	10.70	0.63	0.76	0.79	0.83
10	4.51	5.11	6.12	7.07	0.89	0.94	1.01	1.12
15	3.66	4.04	4.77	5.88	1.06	1.09	1.14	1.20
20	3.18	4.01	4.43	4.99	1.24	1.29	1.36	1.38
25	2.84	3.89	4.42	4.55	1.35	1.47	1.55	1.57

to the pervaporation study, the diffusion coefficients of water as well as acetic acid increased from membrane M to M-3 at all water compositions in the feed. This is attributed to a decrease of cohesive energy of the polymer upon increasing the zeolite content in the membrane matrix, which leads to the increased diffusivity. However, there is a decrease in diffusion coefficients of water for all the membranes by increasing the amount of water in the feed. Such a decrease is quite common at higher compositions of water in the feed because of enhanced swelling behavior of the membrane. On the contrary, diffusion coefficients of acetic acid increased for all the membranes with increasing water composition in feed, a result expected because of deterioration of membrane selectivity toward water at higher compositions of water in the feed. However, the magnitude of acetic acid is quite small compared to that of water, suggesting that the membranes in the present study are selective toward water.

Effect of temperature

The effect of operating temperature on PV performance was studied for all the membranes at 10 mass % of water in the feed and the resulting values are presented in Table IV. It is observed that the permeation rate increased from 30 to 50°C, whereas the separation factor decreased, which is a result of the decreased interaction between permeates, and permeates and membrane at higher temperature, which predominates the plasticizing effect on the membrane. Therefore, the permeation of diffusing molecules and the associated molecules through the membranes become easier, resulting in an increase of total permeation rate, while suppressing the selectivity. However, at lower temperature the transport of water molecules through the membrane matrix is prominent.

The temperature dependency of permeation and diffusion for water can be studied using the Arrhenius-type relationship[12]

$$X = X_0 \exp\left(\frac{-E_x}{RT}\right) \tag{7}$$

where X represents diffusion (D) or permeation (J); X_0 is a constant representing the preexponential factor of D_0 or J_0; and E_x represents activation energy for permeation or diffusion, depending on the transport process under consideration; and RT is the usual energy term. As the feed temperature increases, vapor pressure in the feed compartment also increases, although the vapor pressure at the permeate side is not affected. All these result in an increase of the driving force with increasing temperature.

Arrhenius plots of log J versus $1/T$ and log D versus $1/T$ are shown in Figures 7 and 8 for the temperature dependency of permeation flux and diffusion, respectively. In both cases, linear behavior is observed, suggesting that permeability and diffusivity follow an Arrhenius trend. From least-squares fits of these linear plots, the activation energy values for permeability (E_p) and diffusivity (E_D) were estimated and the results thus obtained are presented in Table V. It is noticed that a pure membrane (M) exhibits higher E_p and E_D values compared to those of zeolite-incorporated membranes (M-1 to M-3). This suggests that

TABLE IV
Pervaporation Flux and separation selectivity at Different Temperatures for Different Membranes at 10 Mass % of Water in the Feed

Temperature (°C)	$J \times 10^2$ (kg m^{-2} h^{-1})				α_{sep}			
	M	M-1	M-2	M-3	M	M-1	M-2	M-3
30	3.44	3.80	4.39	5.00	16.71	17.95	20.03	20.80
40	10.20	10.40	11.60	12.60	12.69	13.36	14.20	14.68
50	25.50	26.20	27.00	29.50	4.43	5.17	6.38	6.87

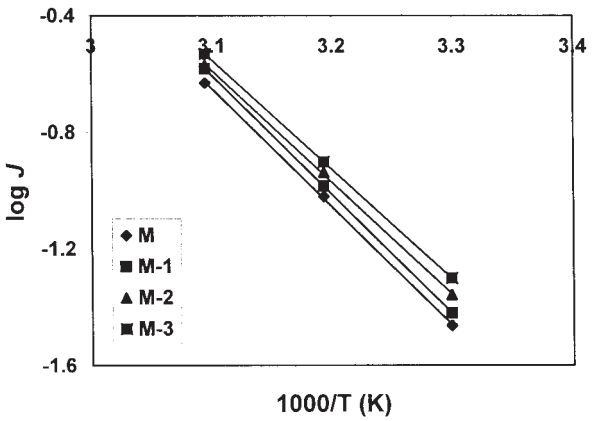

Figure 7 Variation of log J with temperature for different membranes at 10 mass % of water in the feed.

both permeating and diffusing molecules require more energy for transport through the pure membrane (M) because of its dense nature. Obviously, zeolite-incorporated membranes take less energy because of a molecular sieving action attributed to the presence of sodalite cages and super cages in the framework of zeolite.[25] As a result, activation energies for permeation and diffusion decreased systematically from membrane M to M-3 with increasing zeolite content.

Although E_p values are higher than those of E_D values in all the membranes, the difference is not significant, indicating that both permeation and diffusion almost equally contribute to the PV process. The E_p and E_D values ranged between 72.28 and 78.16, and 70.95 and 77.38 kJ/mol, respectively. Using these values, we calculated the heat of sorption as

$$\Delta H_s = E_p - E_D \tag{8}$$

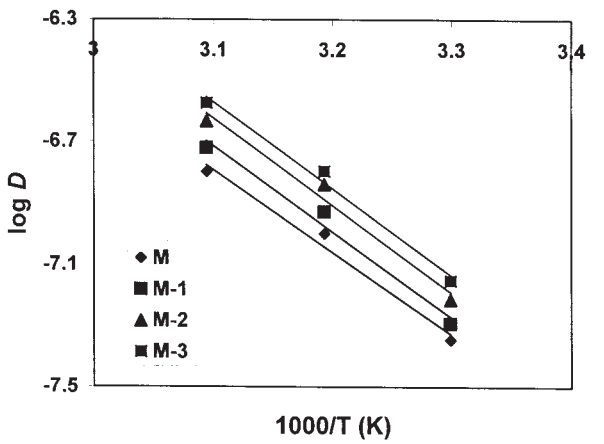

Figure 8 Variation of log D with temperature for different membranes at 10 mass % of water in the feed.

TABLE V
Arrhenius Activation Parameters for Permeation, Diffusion, and Heat of Sorption

Parameter (kJ/mol)	M	M-1	M-2	M-3
E_p	78.16	77.06	73.96	72.28
E_D	77.38	76.11	72.79	70.95
ΔH_s	0.78	0.95	1.17	1.33

The resulting ΔH_s values are included in Table V. The ΔH_s values give the additional information about the transport of molecules through the polymer matrix. It is a composite parameter involving contributions of both Henry-type and Langmuir-type of sorption. Henry's law states that the heat of sorption will be positive for liquid transport, leading to the dissolution of chemical species into that site within the membrane, giving an endothermic contribution to the sorption process. However, Langmuir's sorption requires the preexistence of a site in which sorption occurs by a hole-filling mechanism, giving an exothermic contribution. In the present study, the ΔH_s values obtained are slightly positive for all the membranes, suggesting that Henry's sorption is still predominant, giving an endothermic contribution.

CONCLUSION

Sodium alginate membranes, incorporated with higher amounts of NaY zeolite, showed better performance while separating water–acetic acid mixtures. An increase of zeolite content in the membrane results in a simultaneous increase of both permeation flux and selectivity, attributed to a significant enhancement of hydrophilic character, selective adsorption, and molecular sieving action, including a reduction of pore size of the polymer matrix. The PV separation index data also indicated that the higher the loading of zeolite, the better the membrane performance. The highest separation selectivity was found to be 42.29 with a flux of 3.80×10^{-2} kg m^{-2} h^{-1} for the membrane with the highest loading of zeolite at 30°C for 5 mass % of water composition in the feed. With respect to the temperature effect, the permeation rate increased, while suppressing the selectivity when the temperature was increased, a phenomenon attributed to increasing the predominance of the plasticizing effect on the membrane when the interaction becomes weaker between permeating molecules, permeants, and membrane at higher temperature.

The E_p and E_D values ranged between 72.28 and 78.16, and 70.95 and 77.38 kJ/mol, respectively. The zeolite-incorporated membranes exhibited lower activation energy compared to that of a pure membrane, indicating that the permeants require less energy dur-

ing the process because of molecular sieving action attributed to the presence of sodalite cages and supercages in the framework of zeolite. The almost equal magnitude of E_p and E_D values suggests that both permeation and diffusion contribute equally to the PV process. For all the membranes, Henry's mode of sorption dominates the process, giving an endothermic contribution.

The authors gratefully acknowledge the financial support given by the Department of Science and Technology, New Delhi (Grant SP/S1/H-31/2000), and thank Dr. A. B. Halgeri, Indian Petrochemicals Corp. Ltd., Baroda, India for kindly supplying NaY zeolite.

References

1. Uragami, T.; Okazaki, K.; Matsugi, H.; Miyata, T. Macromolecules 2002, 35, 9156.
2. Kittur, A. A.; Kariduraganavar, M. Y.; Toti, U. S.; Ramesh, K.; Aminabhavi, T. M. J Appl Polym Sci 2003, 90, 2441.
3. Burshe, M. C.; Sawant, S. B.; Joshi, J. B.; Pangarkar, V. G. Sep Purif Technol 1998, 13, 47.
4. Lai, J. Y.; Chen, R. Y.; Lee, K. R. J Appl Polym Sci 1993, 47, 1849.
5. Huang, R. Y. M.; Yeom, C. K. J Membr Sci 1991, 62, 59.
6. Kariduraganavar, M. Y.; Kulkarni, S. S.; Kittur, A. A. J Membr Sci, to appear.
7. Palasantzas, I. A.; Wise, D. L. Resour Conserv Recycl 1994, 11, 225.
8. Dionysiou, D.; Tsianou, M.; Botsaris G. Ind Eng Chem Res 2000, 39, 4192.
9. Han, I. S.; Cheryan, M. Appl Biochem Biotechnol 1996, 19, 57.
10. Huang, R. Y. M.; Moreira, A.; Notarfonzo, R.; Xu, Y. F. J Appl Polym Sci 1988, 35, 1191.
11. Li, S.; Tuan, V. A.; Noble, R. D.; Falconer, J. L. Ind Eng Chem Res 2001, 40, 6165.
12. Huang, R. Y. M.; Yeom, C. K. J Membr Sci 1991, 58, 33.
13. Tsuyumoto, M.; Karakane, H.; Maeda, Y.; Tsgaya, H. Desalination 1991, 80, 139.
14. Ugarami, T.; Takigawa, K. Polymer 1990, 31, 668.
15. Neel, J.; Nguyen, Q. T.; Clement, R.; Lin, D. J. J Membr Sci 1986, 27, 217.
16. Chen, X.; Yang, H.; Gu, Z.; Shao, Z. J Appl Polym Sci 2001, 79, 1144.
17. Yeom, C. K.; Lee, K. H. J Appl Polym Sci 1998, 67, 949.
18. Kurkuri, M. D.; Toti, U. S.; Aminabhavi, T. M. J Appl Polym Sci 2002, 86, 3642.
19. Toti, U. S.; Kariduraganavar, M. Y.; Soppimath, K. S.; Aminabhavi, T. M. J Appl Polym Sci 2002, 83, 259.
20. Yeom, C. K.; Lee, K. H. J Appl Polym Sci 1998, 67, 209.
21. Wang, X. P. J Membr Sci 2000, 170, 71.
22. Gao, Z.; Yue, Y.; Li, W. Zeolites 1996, 16, 70.
23. Jia, M. D.; Peinemann, K. V.; Behling, R. D. J Membr Sci 1991, 57, 289.
24. Kim, K. J.; Park, S. H.; So, W. W.; Moon, S. J. J Appl Polym Sci 2000, 79, 1450.
25. Kariduraganavar, M. Y.; Kittur, A. A.; Kulkarni, S. S. J Membr Sci 2004, 238, 165.
26. Hu, H. L.; Lee, K. R.; Lai, J. Y. J Macromol Sci Pure Appl Chem A 1993, 30, 815.
27. Lee, K. R.; Chen, R. Y.; Lai, J. Y. J Membr Sci 1992, 75, 171.
28. Lee, Y. M.; Bourgeois, D.; Belfort, G. J Membr Sci 1989, 44, 161.
29. Cabasso, I.; Jagu-Grodzinski, J.; Vofsi, D. J Appl Polym Sci 1974, 18, 2137.
30. Hwang, S. T; Kammermeyer, K. Membrane in Separations; Wiley–Interscience: New York, 1975.
31. Yamasaki, A.; Iwatsubo, T.; Masuoka, T.; Misoguchi, K. J Membr Sci 1994, 89, 111.
32. Kusumocahyo, S. P.; Sudoh, M. J Membr Sci 1999, 161, 77.